

New insights in large-pores mesoporous silica microspheres for hemostatic application

*Original*

New insights in large-pores mesoporous silica microspheres for hemostatic application / Mohamed, Sara Saber Younes; Cavalli, Roberta; Rombi, Elisabetta; Atzori, Luciano; Armandi, Marco; Onida, Barbara. - In: JOURNAL OF MATERIALS SCIENCE. MATERIALS IN MEDICINE. - ISSN 1573-4838. - ELETTRONICO. - 36:1(2025), pp. 1-9. [10.1007/s10856-025-06864-9]

*Availability:*

This version is available at: 11583/2997459 since: 2025-02-11T11:28:10Z

*Publisher:*

SPRINGER

*Published*

DOI:10.1007/s10856-025-06864-9

*Terms of use:*

This article is made available under terms and conditions as specified in the corresponding bibliographic description in the repository

*Publisher copyright*

(Article begins on next page)



Original Research

# New insights in large-pores mesoporous silica microspheres for hemostatic application

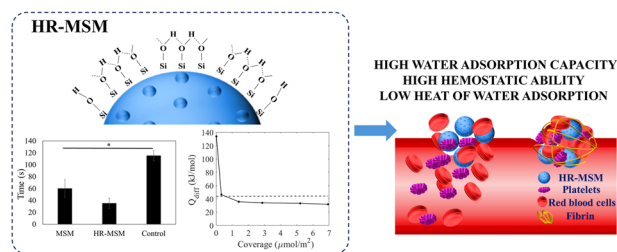
Sara Saber Younes Mohamed<sup>1</sup> · Roberta Cavalli<sup>2</sup> · Elisabetta Rombi<sup>3</sup> · Luciano Atzori<sup>3</sup> · Marco Armandi<sup>1</sup> · Barbara Onida<sup>1</sup>

Received: 3 July 2024 / Accepted: 22 January 2025  
© The Author(s) 2025

## Abstract

Hemorrhages are still considered a common cause of death and despite the availability of different hemostatic agents it is still necessary to develop more effective hemostats for bleeding managements in emergency situations. Herein, large-pores mesoporous silica microspheres (MSM) were synthesized, and their surface was modified to enrich the hydroxyls population with the aim of achieving a material with enhanced water adsorption capacity and high hemostatic ability. The success of surface modification was investigated by Fourier Transform Infrared spectroscopy (FT-IR) and thermogravimetric analysis (TGA), which confirmed the increase in the amount of surface hydroxyl groups. A hemolysis assay as well as a clotting test were carried out to evaluate the hemocompatibility and hemostatic ability, respectively. It was found that the modified material presented the lowest hemolytic ratio and the lowest clotting time. The novelty of the paper is mainly due to the coupling of the hemostatic ability test with the adsorption microcalorimetry of water. In fact, being the water adsorption on the material surface a crucial factor in the hemostatic activity, microcalorimetry was used for the first time to study the adsorption of water and estimate its heat of adsorption. The data obtained showed that the modified MSM presents a surface able to adsorb a higher amount of water, compared to the pristine MSM, with a low molar heat of adsorption (about 35 kJ/mol), which renders the modified MSM presented in the present study an excellent candidate for producing novel hemostats.

## Graphical Abstract



## 1 Introduction

Hemorrhages and their complications are considered one of the most common causes of potentially preventable death among injured patients either in the military or in the civilian field. Indeed, it has been estimated that severe blood loss remains the main responsible of about 50% of battlefield victims, 20% of trauma death in civilian hospitals, and 30% of maternal mortality [1, 2]. Beyond causing death, uncontrolled bleeding can lead to other severe consequences such as impair wound healing, infections, coagulopathy and organ failure [3]. Therefore, efficient and rapid bleeding control results of great importance to decrease the risk of

✉ Sara Saber Younes Mohamed  
sara.mohamed@polito.it

<sup>1</sup> Department of Applied Science and Technology, Polytechnic of Turin, Turin, Italy  
<sup>2</sup> Department of Drug Science and Technology, University of Turin, Turin, Italy  
<sup>3</sup> Department of Chemical and Geological Sciences, University of Cagliari, Monserrato, Cagliari, Italy

mortality during pre-hospital treatments. Various hemostatic biomaterials, based on both organic (for example, chitosan and gelatin) and inorganic (for example, zeolites and clays) materials, have been developed for bleeding management. Compared to organic materials, inorganic materials have been recommended in the management of massive bleeding as they exhibit unique properties, such as high porosity, which make them able to quickly adsorb water and achieve rapid hemostasis. However, the use of these materials has been limited as they present some adverse side effects, such as thermal damage and necrosis to the tissues surrounding the injuries due to the exothermic reaction following water adsorption and abnormal foreign-body reaction due to their poor biodegradability [4–6]. Because of these limitations, there is still a need for the search of alternative materials able to control hemorrhages and reduce collateral effects. Mesoporous silica (MS) has recently gained much attention in the field of hemostasis because of its unique physico-chemical properties including tailorable surface, high porosity, and biocompatibility. Several studies have investigated the influence of MS properties on its hemostatic ability [7–14]. From the analysis of the literature, it emerged that the hemostatic ability of MS is mainly attributed to its large pores and high surface area, which enhances its adsorption capacity of water from the blood, condensing platelets, blood cells, and clotting factors at the bleeding site (factor concentrator mechanism). Another fact that might be beneficial for blood coagulation is the negative charges formed on the surface of MS materials immersed in the biological fluid, which can activate factor XII and other clotting factors (procoagulant effect) [1, 4, 11]. Finally, the presence of hydroxyl groups on the surface of MS can facilitate the wettability of the material in the blood through the formation of intermolecular hydrogen bonds with water molecules, favoring the contact between the MS and the blood [15].

Considering the above premises, the aim of the present study is, on the one hand, the fabrication of large-pores mesoporous silica microspheres (MSM) with a high density of hydroxyl groups and enhanced water adsorption capacity, to be used in the management of massive bleeding, as they should present high hemostatic ability. To this purpose, MSM with large pores, previously studied as a hemostatic material [14], were synthesized and their surface was modified in order to increase the density of hydroxyl groups aiming to obtain a material with enhanced water adsorption capacity. To investigate the effect of surface modification, different techniques, such as Fourier Transform Infrared spectroscopy (FT-IR) and thermogravimetric analysis (TGA), were used to characterize the material. A clotting time test as well as a hemolysis assay were performed to evaluate the hemostatic ability and hemocompatibility, respectively.

On the other hand, considering the crucial role of the interaction of the material with water in the hemostatic activity, the study of water adsorption on the silica surface appears fundamental. Besides the characterization of its water adsorption capacity, the knowledge of the heat of adsorption of water is particularly relevant. Indeed, the use of inorganic hemostats based on zeolites (*i.e.*, QuikClot™) has been limited as it was observed that they caused thermal injury of the surrounding tissue at the bleeding site. It is believed that these injuries can be related to the adsorption of water by zeolites, which is known to be highly exothermic and which can increase the temperature of local tissue surface up to 90 °C, causing severe damage [4]. Therefore, in the present study, microcalorimetry was employed to study the adsorption of water and estimate its heat of adsorption on modified MSM. To the best of authors' knowledge, this is the first time that the investigation of the hemostatic and hemolytic activities of mesoporous silica particles is complemented by the study of water adsorption on the material surface, so obtaining new insights concerning their potential use as a novel hemostatic material.

## 2 Experimental section

### 2.1 Materials

Pluronic P123, potassium chloride (KCl, ≥99,0%), hydrochloric acid (ACS reagent, 37%), mesitylene (98%), tetraethyl orthosilicate (TEOS, 99.999% trace metals basis), and potassium hydroxide were purchased from Sigma-Aldrich (St. Louis, MO, USA). Water (LC-MS grade) was acquired from Merck (Billerica, MA, USA).

### 2.2 Synthesis and surface modification of mesoporous silica microspheres

The mesoporous silica microspheres (MSM) were synthesized according to the procedure reported by the authors in a previous paper [14] except for the amount of reactants, which was doubled. In brief, 8.0 g of Pluronic P123 and 12.2 g of KCl were dissolved in a mixture of 240 g of H<sub>2</sub>O (LC-MS grade) and 47.2 g of HCl (37% w/w); then 6.0 g of mesitylene were added and the solution was stirred. After 2 h of stirring, 17 g of TEOS was added dropwise and the mixture was stirred vigorously for 10 min. The molar ratios of the reactants were 1 TEOS:0.017 P123:0.6 mesitylene:2 KCl:5.85 HCl:165 H<sub>2</sub>O. The mixture was maintained at 35 °C under static condition for 24 h, then it was transferred into a sealed PTFE bottle and kept at 100 °C for 24 h. The resulting precipitate was filtered, washed with distilled water, and dried at 60 °C in an oven for one night. The dried

material was calcined in air at 500 °C for 6 h at a heating rate of 15 °C/min in a muffle furnace to remove the template.

In order to enrich the hydroxyls population of MSM, the sample was treated with two aqueous solutions, i.e. 1 M HCl for 24 h and 0.01 M KOH for 2 h, according to the procedures reported in previous studies [16, 17]. For the first treatment, 800 mg of MSM were suspended in 24 ml of 1 M HCl solution, under constant stirring, at 25 °C for 24 h. Then, the resulting powder was filtered, washed with distilled water, and dried at 60 °C in an oven for one night. For the second treatment, 600 mg of the previously treated powder were dispersed in 7.5 ml of water (LC-MS grade) by sonication. Then, 225 ml of 0.01 M KOH solution were added, and the mixture was stirred at 250 rpm for 2 h. The precipitate was separated by centrifugation and washed with distilled water (this procedure was repeated for three times). Finally, the solid was dried at 60 °C in an oven until complete evaporation of the solvent. The obtained material, which is a hydroxyls-rich large-pores mesoporous silica, is hereafter named HR-MSM.

### 2.3 Instrumental characterization

Samples morphology was characterized using a Field Emission Scanning Electron Microscope (FESEM ZEISS Merlin instrument, Oxford Instruments, Abingdon-on-Thames, UK). The samples were mounted on a metal stub with double-sided adhesive tape and coated with platinum before the analysis.

Textural properties of the sample were determined by N<sub>2</sub> adsorption-desorption at 77 K, using a Micromeritics ASAP 2020 Plus Physisorption analyzer (Micromeritics, Norcross, GA, USA). Before the measurement, the samples were outgassed at 150 °C for 2 h. The specific surface area (SSA) was calculated using the Barret-Emmett-Teller (BET) method in the relative pressure range of 0.11–0.30. The total pore volume (V<sub>p</sub>) was determined at a relative pressure of about 0.90. The pore size distribution and the average pore size (D<sub>p</sub>) were obtained using the density functional theory (DFT) model.

X-ray photoelectron spectroscopy (XPS) was carried out on a Physical Electronics VersaProbe instrument (Physical Electronics, Lake Drive, MN, USA), using Al radiation.

Fourier Transform Infrared (FT-IR) analysis was carried out on self-supported pellets using an Equinox 55 spectrometer (Bruker, Billerica, MA, USA). The pellets were prepared by pressing the powder with a hydraulic press. All samples were outgassed in high vacuum (residual pressure equal to 0.1 Pa) at room temperature for 30 min. Spectra were recorded from 4000 cm<sup>-1</sup> to 600 cm<sup>-1</sup> with a resolution of 2 cm<sup>-1</sup>.

TG analysis was carried out in argon flow on a Linseis STA PT 1600 (TGA-DSC) instrument (LINSEIS Co.

Germany) between 25 °C and 600 °C at the heating rate of 10 °C/min.

### 2.4 Hemolysis assay

The hemolytic activity was evaluated on rat blood diluted with PBS pH 7.4 (1:10 v/v), according to the procedure reported in [14]. Briefly, 100 µl of the sample prepared in saline solution (NaCl 0.9% w/v) was incubated with 900 µl of diluted blood at 37 °C for 90 min, so that the final concentration was 1 mg/ml. After incubation, the samples were centrifuged at 6000 rpm for 12 min to separate the plasma. The amount of hemoglobin released in the supernatant due to hemolysis was measured spectrophotometrically at 542 nm (Du 730 spectrophotometer, Beckman).

The hemolytic activity was calculated with reference to complete hemolyzed samples (induced by the addition of Triton X-100 1% w/v to the blood, used as positive control) and negative control (NaCl 0.9% w/v).

$$\text{Hemolysis}(\%) = \frac{(\text{Abs sample} - \text{Abs neg})}{(\text{Abs pos} - \text{Abs neg})} \times 100$$

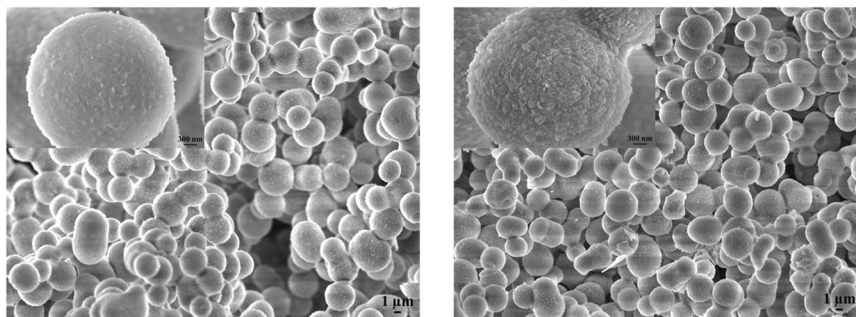
### 2.5 In vitro blood coagulation test

Clotting time (CT) test is a simple method used to evaluate whole blood coagulation in vitro. The hemostatic ability of the samples was evaluated on 3.2% sodium citrate rat blood diluted (1:3 v/v) with saline solution (NaCl 0.9% w/v) according to the procedure reported in literature [11, 12]. Briefly, 2 mg of powder were put in an eppendorf tube and kept at 37 °C for 5 min. Then 200 µl of diluted blood was added to the powder, followed by vortexing for 10 s, and incubated at 37 °C for 3 min. After that, 100 µl of 0.025 M calcium chloride (CaCl<sub>2</sub>) aqueous solution was added to the tube to activate blood coagulation. Finally, the tube was tilted every 15 s until the blood stopped to flow through the wall of the tube. The clotting time was used as the result of the CT test.

### 2.6 Microcalorimetry of water adsorption

The microcalorimetric measurements were performed by using a Tian-Calvet heat flow calorimeter (Setaram) equipped with a volumetric vacuum line. Before the analysis, the sample (ca. 0.1 g, 40–60 mesh) was evacuated at 150 °C for 12 h under vacuum (ca. 2 × 10<sup>-3</sup> Pa). The analysis was carried out at 30 °C admitting successive doses of water previously degassed by using the freeze-pump-throw procedure. For each dose, the equilibrium pressure was measured by means of a differential pressure gauge (Leybold) and the thermal effect was recorded. The analysis was stopped at a final equilibrium pressure of ca. 800 Pa. Using

**Fig. 1** FESEM images (magnification: 5.00 K X and 50.00 K X in the inset) of MSM (left side) and HR-MSM (right side)



the data collected from the measurements, both the volumetric isotherm (relating the amount of water adsorbed with the corresponding equilibrium pressure) and the calorimetric isotherm (relating the integral heat of adsorption with the corresponding equilibrium pressure) were drawn. Combining the two sets of data, a plot of the differential heat of adsorption as a function of the adsorbed water amount was obtained, which gives information on the influence of the surface coverage on the energetics of the adsorption.

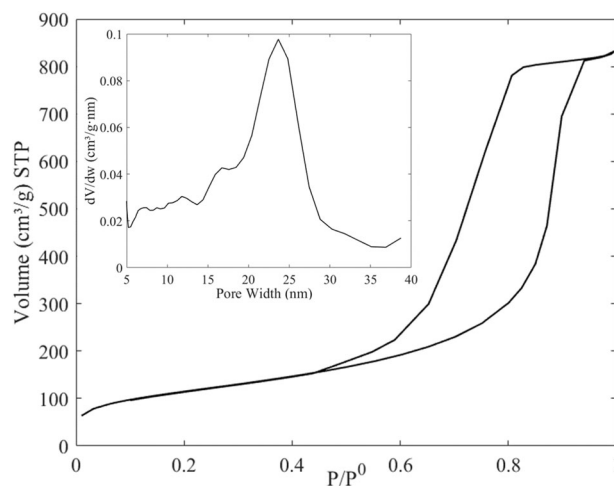
### 3 Results and discussion

#### 3.1 Characterization of HR-MSM

FESEM images of MSM and HR-MSM are reported in Fig. 1. The synthesized material (Fig. 1, left side) appears in the form of spheres with particle size ranging from 1.5 to 5  $\mu\text{m}$  as previously observed [14]. As far as sample HR-MSM (Fig. 1, right side) is concerned, no remarkable changes can be observed in the morphology when compared to the as-synthesized material (Fig. 1, left side). However, a rough surface might be observed in the case of HR-MSM (Fig. 1, right side, inset), whereas this is not so evident for MSM as such (Fig. 1, left side, inset). The rough surface could be ascribed to the partial dissolution of silica due to the treatment with the basic solution (0.01 M KOH solution) during the surface modification process, as observed previously [18, 19].

Nitrogen adsorption-desorption isotherms and pore size distribution of HR-MSM are shown in Fig. 2. The material exhibits a type IV isotherm, according to IUPAC classification, with a hysteresis loop which appears of type H1, typical of a narrow range of uniform mesopores [20]. Indeed, the pore size distribution (Fig. 2, inset) is unimodal and centered at 24 nm. The values of  $\text{SSA}_{\text{BET}}$  and  $V_p$  are 415  $\text{m}^2/\text{g}$  and 1.19  $\text{cm}^3/\text{g}$ , respectively. All these features can be considered comparable to the data previously reported in [14].

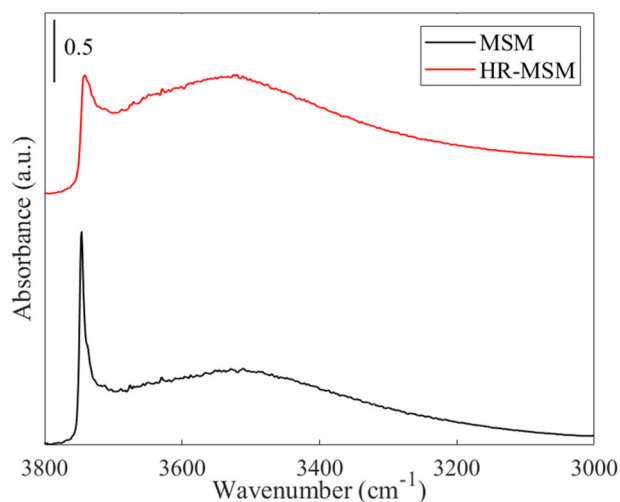
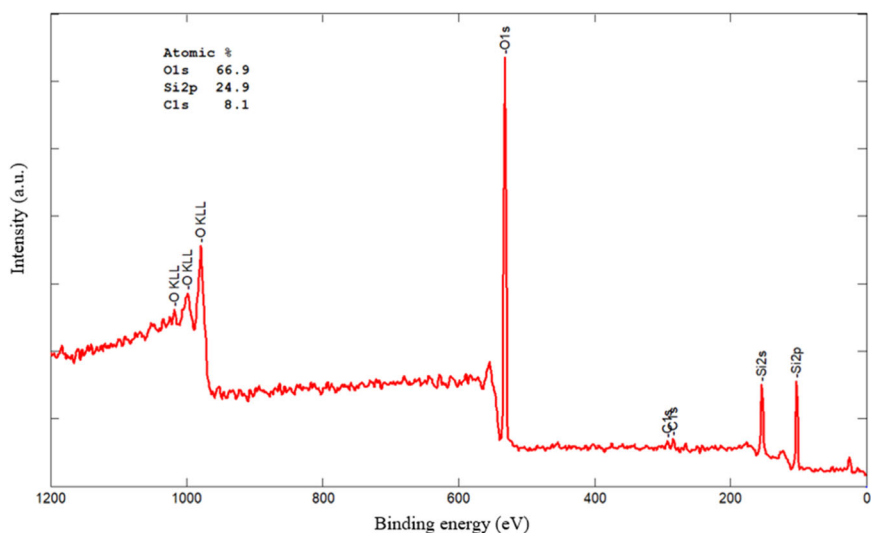
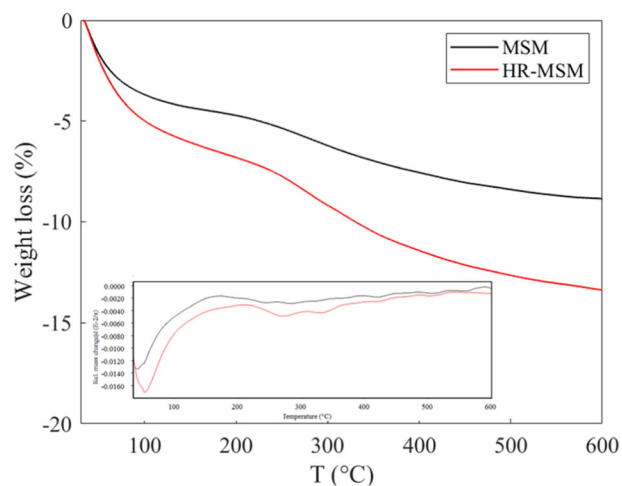
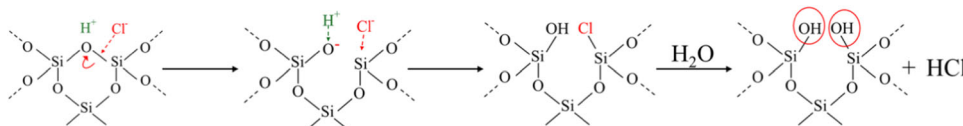
XPS analysis was carried out to exclude the presence of chlorine and potassium on the surface of HR-MSM as



**Fig. 2** Nitrogen adsorption-desorption isotherms of HR-MSM and pore size distribution (inset)

residual contaminants due to the treatments in aqueous solutions. The result of the survey analysis, reported in Fig. 3, evidenced that Si and O are the main elements at the surface, as expected. Traces of carbon are also observed, as usual, which are ascribed to organic impurities adsorbed during the handling and storage of the sample.

The FT-IR spectroscopic characterization was performed to evidence the effect of the treatments in the acidic and basic solutions on the population of hydroxyl groups at the surface. Figure 4 reports the spectrum of HR-MSM, with that of the pristine MSM for comparison. The spectrum of MSM is the typical spectrum of amorphous silica, as previously reported [14], showing two main bands, i.e. a narrow one due to stretching of isolated silanols, observed at 3746  $\text{cm}^{-1}$ , and a broad band centered at about 3520  $\text{cm}^{-1}$  due to H-bonded silanols [21]. As far as the spectrum of HR-MSM (Fig. 4, red spectrum) is concerned, the relative intensities of the two contributions are significantly different from those observed for MSM, so that the spectrum suggests that the population of H-bonded silanols increased and that of isolated silanols decreased in HR-MSM respect to the pristine MSM. This modification of the surface silanols population is ascribed to the hydrolysis of siloxane bridges, caused by the treatments in acidic and basic

**Fig. 3** XPS spectrum (survey) of HR-MSM**Fig. 4** FT-IR Spectra of HR-MSM (red curve) and of pristine MSM (black curve)**Fig. 5** TG and DTG (inset) Curves of MSM (black curve) and HR-MSM (red curve)**Scheme 1** A possible reaction occurring on the surface of MSM in acidic solution (inspired by El Mourabit et al. [22])

solutions, which formed new SiOH species. A possible mechanism of reaction in acidic solution, as proposed in [22], is reported in Scheme 1.

The reaction in basic solution is expected to be that responsible of incipient silica dissolution which is well known, as reported, for instance, in [23].

In order to obtain a quantitative estimation of silanols population, TGA analysis was performed on both pristine MSM and HR-MSM and Fig. 5 reports the obtained curves.

For both samples, two main weight loss can be observed. A first one, at temperatures lower than 150 °C, which can be assigned to the removal of adsorbed molecular water weakly interacting with the surface, and a second one, at temperatures higher than 200 °C, ascribed to the condensation of silanols groups on the silica surface [24]. As far as sample HR-MSM is concerned, it can be observed that the first weight loss (about 6.1 wt%) and the second weight loss (about 7.3 wt%) are both larger than those observed for

MSM (about 4.3 wt% and 4.5 wt%, respectively). The larger weight loss due to the removal of adsorbed molecular water observed for HR-MSM suggests a higher capacity of water adsorption when compared to MSM. Moreover, an estimation of the surface density of hydroxyl groups was performed using the weight loss between 200 °C and 600 °C, according to the following equation:

$$OH/nm^2 = \frac{\Delta m_{(T2-T1)} \times N_A}{SSA_{BET} \times m_{T1}} \times 2$$

where  $\Delta m_{(T2-T1)}$  is the weight loss between T1 (200 °C) and T2 (600 °C),  $N_A$  is Avogadro's constant,  $MW_{H_2O}$  is the molecular weight of water,  $m_{T1}$  is the sample weight at T1, and  $SSA_{BET}$  is the specific surface area [25].

The number of silanol groups per square nanometer ( $OH/nm^2$ ) was found to be about 5 and 11 for pristine MSM and HR-MSM, respectively.

The value obtained for MSM is comparable with the data previously reported for mesoporous silica synthesized using the same templating agent (Pluronic P123) in acidic conditions, such as SBA-15 [26], also considering the limitations, in terms of precision and accuracy, of the measure of the number of hydroxyls by thermogravimetric analysis.

The TGA results reveal that the treatments in acidic and basic solutions caused a drastic increase in the amount of silanols, leading to a surface with an increased water adsorption capacity, as desired.

### 3.2 Hemolysis assay

Since it is known that silica could cause damage to the membrane of red blood cells [27, 28], a hemolysis assay was performed to evaluate the hemolytic behavior of MSM and HR-MSM. Figure 6 reports the hemolysis ratio of MSM and HR-MSM at a concentration of 1 mg/ml. The results of the test showed that the hemolytic ratio was low for both samples. In particular, HR-MSM presented the lowest value, suggesting that the surface modification may have reduced the hemolytic activity of MSM. A similar result was observed by Shi et al. [29] who studied the effect of silica surface modification, performed by treating silica with HCl and  $NH_4OH$ , on hemolysis. The authors suggested that the reduced hemolytic activity might be ascribed to the modification of the silica surface in the basic solution. A gel-like layer or the hydration of the particles may cause a steric repulsion between the particles and the red blood cells, explaining the low hemolysis after alkaline treatment.

### 3.3 Clotting time test

To evaluate the hemostatic ability of MSM and HR-MSM, a clotting time (CT) test was performed. As reported in Fig. 7,

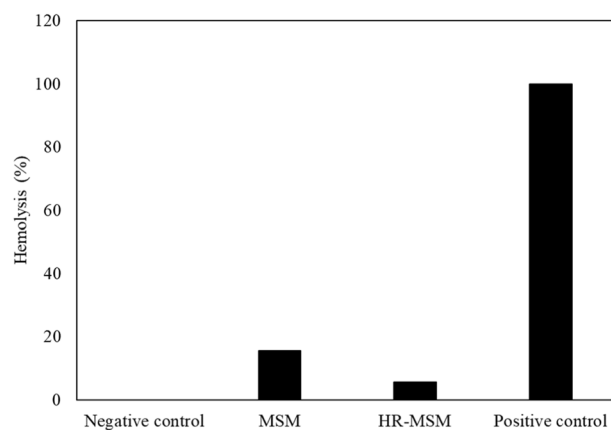


Fig. 6 Hemolytic activity of MSM and HR-MSM

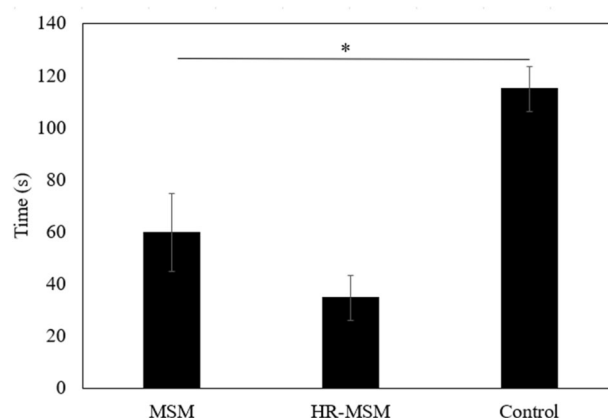


Fig. 7 CT for MSM, HR-MSM, and control. Data are represented as mean  $\pm$  SD ( $n = 3$ ). \* Significant difference ( $p < 0.05$ ) analyzed by one-way ANOVA

the clotting times of MSM ( $60 \text{ s} \pm 15 \text{ s}$ ) and HR-MSM ( $35 \text{ s} \pm 9 \text{ s}$ ) were significantly shorter than the control ( $115 \text{ s} \pm 9 \text{ s}$ ), where no material was used. In addition, it can be observed that the CT of HR-MSM was the shortest. This could be ascribed to the fact that the HR-MSM sample may present a higher water adsorption capacity when compared to MSM, which might have enhanced its hemostatic ability by accelerating blood clotting [5], as desired.

### 3.4 Microcalorimetric characterization of water adsorption

With the aim of obtaining a more detailed picture of the silica surface role in the hemostatic activity, with particular reference to the propensity of adsorbing the water molecules, the adsorption of water was studied by microcalorimetry, from which both the volumetric and the calorimetric isotherms were obtained.

Figure 8 reports the volumetric isotherm of HR-MSM, previously outgassed at 150 °C in order to remove the adsorbed molecular water (according to TGA analysis,

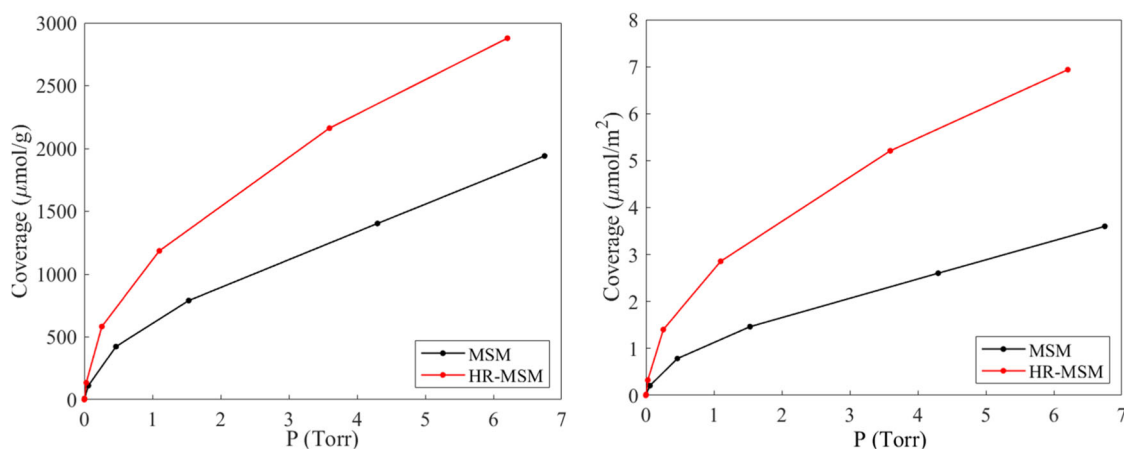


**Fig. 8** Volumetric isotherms of water adsorbed on MSM and HR-MSM at 30 °C, where coverage is expressed per unit mass (left side) and per unit surface area (right side)

Fig. 5), compared to that obtained for the pristine MSM.

The water uptake is definitely larger for HR-MSM than for MSM and when the quantities of water adsorbed at similar equilibrium pressures are compared per unit surface area, the amount observed for HR-MSM appears about twice that measured for MSM (Fig. 8, right side). Interestingly, the ratio between the amounts of water adsorbed on the two samples is close to the ratio between the numbers of silanols estimated by TGA analysis (11 : 5, Fig. 5).

These results corroborate the scenario previously proposed, for which the enhanced water adsorption capacity of HR-MSM (as suggested by TGA data) is due to the high silanols surface density obtained by the treatment in acidic and basic solutions, this feature being responsible for the enhanced hemostatic ability observed by the CT (Fig. 7).

Therefore, HR-MSM can indeed be considered an optimal candidate for hemostatic applications. For this reason, microcalorimetric isotherms were used to estimate the heat of adsorption. In fact, as already highlighted, the heat of water adsorption could be the cause of thermal injury of the surrounding tissue at the bleeding site when inorganic materials such as zeolites are used as hemostats [4].

Microcalorimetry has been widely applied to investigate the thermodynamics of water adsorption on both crystalline and amorphous silicas, in order to evaluate the energy of the interaction between the surface and water molecules [30]. This parameter appears crucial in affecting several surface properties of silicas and silica-based materials, which may be even more significant when the interaction with biological environments is conceived for the material [28, 31].

Figure 9 reports the molar heat of adsorption on HR-MSM as a function of water coverage, i.e. the differential heat of adsorption ( $Q_{\text{diff}}$ ) [30, 32]. It can be noted that, starting from a value of 134 kJ/mol at negligible coverage (ascribed to traces of strong adsorption sites usually

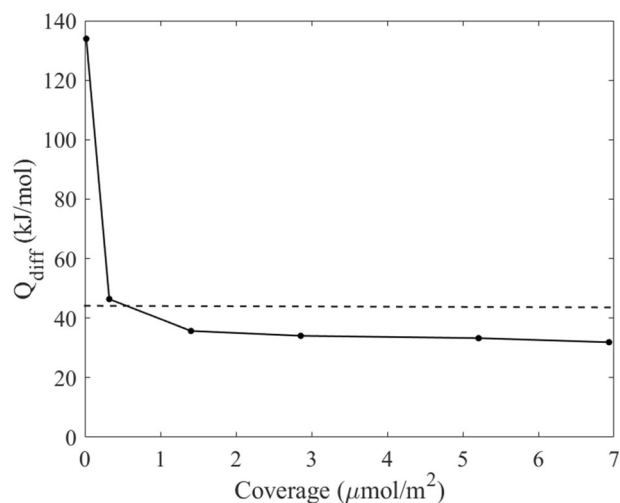


**Fig. 9** Differential heat ( $Q_{\text{diff}}$ , kJ/mol) of water adsorption on HR-MSM as a function of coverage. The sample was previously outgassed at 150 °C

observed in amorphous silicas [24, 25]),  $Q_{\text{diff}}$  abruptly decreases below 44 kJ/mol (dashed line in Fig. 9), i.e. the latent enthalpy of liquefaction of water, at very low coverages ( $0.56 \mu\text{mol/m}^2$ , corresponding to  $0.34 \text{ molecules/nm}^2$ ), reaching a quasi-plateau at about 35 kJ/mol (remarkably lower than the latent enthalpy of liquefaction of water) for adsorbed amounts above  $1.4 \mu\text{mol/m}^2$  (corresponding to  $0.84 \text{ molecules/nm}^2$ ). This trend clearly indicates that the energy of the interaction of water with the surface is lower than in the liquid phase, at variance with what observed for zeolites, for which values of  $Q_{\text{diff}}$  between 80 and 60 kJ/mol were measured at equilibrium pressures similar to the present ones, i.e. 1–7 Torr [32]. Interestingly, also for all-silica zeolitic materials, the  $Q_{\text{diff}}$  values resulted higher than those measured for HR-MSM, being larger than 44 kJ/mol in the same range of equilibrium pressures [32].

The whole set of data obtained by the characterization of water adsorption on HR-MSM reveal that this material exposes a surface which is able to adsorb an enhanced amount of water with respect to the pristine MSM, and that the energy of adsorption is significantly lower than that measured for zeolites (and even lower than the latent enthalpy of liquefaction of water), hence showing that the large-pores mesoporous silica microspheres herein presented may be an ideal candidate for producing novel hemostats.

## 4 Conclusions

The present work dealt with the fabrication of large-pores mesoporous silica with a high density of hydroxyl groups and enhanced water adsorption capacity to be used in the management of massive bleeding. To this purpose, MSM (with an average pore diameter of 24 nm) were synthesized and treated with two aqueous solutions (i.e. 1 M HCl for 24 h and 0.01 M KOH for 2 h) to enrich the surface hydroxyls population. FT-IR analysis revealed the presence of a relative higher population of H-bonded silanols and a relative lower population of isolated silanols for the treated material (HR-MSM) than for the pristine MSM, suggesting that the treatment may have caused the hydrolysis of siloxane bridges and the formation of new SiOH species. The same result was also confirmed by TGA where an increased amount of silanols was observed for HR-MSM with respect to pristine MSM. To evaluate the hemolytic behavior of MSM and HR-MSM, a hemolysis assay was performed. The results of the test showed that HR-MSM presented the lowest hemolytic ratio, and this may be due to the presence of a more negative charged surface (when immersed in blood) that increased the electrostatic repulsion between net negatively charged red blood cells and the silica surface. A clotting time test was performed to evaluate the hemostatic ability of samples. It was observed that the clotting time of HR-MSM was the shortest, which could be ascribed to the presence of a higher water adsorption capacity of HR-MSM, which might have enhanced its hemostatic ability by accelerating blood clotting. Microcalorimetry was employed to study the adsorption of water and to estimate its heat of adsorption on HR-MSM. The isotherm of HR-MSM showed a larger water uptake for HR-MSM than for pristine MSM, which may explain the enhanced hemostatic ability observed by the clotting time test. The differential heat of adsorption of HR-MSM was about 35 kJ/mol, which is lower than the value measured for other inorganic materials used as hemostats, such as zeolites, and even lower than the latent enthalpy of liquefaction of water.

In conclusion, the results reported in this study show that HR-MSM can be considered a promising candidate for developing new hemostats to be used for bleeding management in emergency situations.

## Compliance with ethical standards

**Conflict of interest** The authors declare no competing interests.

**Publisher's note** Springer Nature remains neutral with regard to jurisdictional claims in published maps and institutional affiliations.

**Open Access** This article is licensed under a Creative Commons Attribution-NonCommercial-NoDerivatives 4.0 International License, which permits any non-commercial use, sharing, distribution and reproduction in any medium or format, as long as you give appropriate credit to the original author(s) and the source, provide a link to the Creative Commons licence, and indicate if you modified the licensed material. You do not have permission under this licence to share adapted material derived from this article or parts of it. The images or other third party material in this article are included in the article's Creative Commons licence, unless indicated otherwise in a credit line to the material. If material is not included in the article's Creative Commons licence and your intended use is not permitted by statutory regulation or exceeds the permitted use, you will need to obtain permission directly from the copyright holder. To view a copy of this licence, visit <http://creativecommons.org/licenses/by-nc-nd/4.0/>.

## References

1. Pourshahrestani S, Kadri NA, Zeimaran E, Towler MR. Well-ordered mesoporous silica and bioactive glasses: promise for improved hemostasis. *Biomater Sci.* 2019;7:31–50. <https://xlink.rsc.org/?DOI=C8BM01041B>.
2. Weeks A. The prevention and treatment of postpartum haemorrhage: what do we know, and where do we go to next? *BJOG Int J Obstet Gynaecol.* 2015;122:202–10. <https://obgyn.onlinelibrary.wiley.com/doi/10.1111/1471-0528.13098>.
3. Schreiber MA, Neveleff DJ. Achieving hemostasis with topical hemostats: making clinically and economically appropriate decisions in the surgical and trauma settings. *AORN J.* 2011;94:S1–20. <https://doi.org/10.1016/j.aorn.2011.09.018>.
4. Pourshahrestani S, Zeimaran E, Djordjevic I, Kadri NA, Towler MR. Inorganic hemostats: The state-of-the-art and recent advances. *Mater Sci Eng C.* 2016;58:1255–68. <https://linkinghub.elsevier.com/retrieve/pii/S0928493115303325>.
5. Zheng Y, Wu J, Zhu Y, Wu C. Inorganic-based biomaterials for rapid hemostasis and wound healing. *Chem Sci.* 2023;14:29–53. <http://xlink.rsc.org/?DOI=D2SC04962G>.
6. Shao H, Wu X, Deng J, Yang Y, Chen W, Li K, et al. Application and progress of inorganic composites in haemostasis: a review. *J Mater Sci.* 2024; Available from: <https://link.springer.com/10.1007/s10853-024-09595-4>.
7. Baker SE, Sawvel AM, Fan J, Shi Q, Strandwitz N, Stucky GD. Blood clot initiation by mesocellular foams: dependence on nanopore size and enzyme immobilization. *Langmuir.* 2008;24:14254–60. <https://pubs.acs.org/doi/10.1021/la802804z>.
8. Dai C, Yuan Y, Liu C, Wei J, Hong H, Li X, et al. Degradable, antibacterial silver exchanged mesoporous silica spheres for hemorrhage control. *Biomaterials.* 2009;30:5364–75. <https://doi.org/10.1016/j.biomaterials.2009.06.052>.
9. Wu X, Wei J, Lu X, Lv Y, Chen F, Zhang Y, et al. Chemical characteristics and hemostatic performances of ordered mesoporous calcium-doped silica xerogels. *Biomed Mater.* 2010;5:035006.
10. Hong H, Wang C, Yuan Y, Qu X, Wei J, Lin Z, et al. Novel porous silica granules for instant hemostasis. *RSC Adv.* 2016;6:78930–5. <https://doi.org/10.1039/C6RA13999J>.

11. Chen Z, Li F, Liu C, Guan J, Hu X, Du G. et al. Blood clot initiation by mesoporous silica nanoparticles: Dependence on pore size or particle size? *J Mater Chem B*. 2016;4:7146–54. <https://xlink.rsc.org/?DOI=C6TB01946C>.
12. Wang C, Zhou H, Niu H, Ma X, Yuan Y, Hong H. et al. Tannic acid-loaded mesoporous silica for rapid hemostasis and antibacterial activity. *BiomaterSci*. 2018;6:3318–31. <https://doi.org/10.1039/c8bm00837j>.
13. Zhang Z, Liu T, Qi Z, Li F, Yang K, Ding S, et al. Fabrication of effective mesoporous silica materials for emergency hemostasis application. *Silicon*. 2022;14:10521–34. <https://link.springer.com/10.1007/s12633-021-01648-6>.
14. Mohamed SSY, Gambino A, Banchemo M, Ronchetti S, Manna L, Cavalli R, et al. Tranexamic acid-loaded mesoporous silica microspheres as a hemostatic material. *Mater Today Commun*. 2023;34:105198. <https://linkinghub.elsevier.com/retrieve/pii/S2352492822020396>.
15. Li X-F, Lu P, Jia H-R, Li G, Zhu B, Wang X, et al. Emerging materials for hemostasis. *Coord Chem Rev*. 2023;475:214823. <https://linkinghub.elsevier.com/retrieve/pii/S0010854522004180>.
16. Suárez Barrios M, de Santiago Buey C, García Romero E, Martín Pozas JM. Textural and structural modifications of saponite from Cerro del Aguila by acid treatment. *Clay Miner*. 2001;36:483–8. [https://www.cambridge.org/core/product/identifier/S0009855800022925/type/journal\\_article](https://www.cambridge.org/core/product/identifier/S0009855800022925/type/journal_article).
17. Chandra P, Doka DS, Umbarkar SB, Vanka K, Biradar AV. Silica microspheres containing high density surface hydroxyl groups as efficient epoxidation catalysts. *RSC Adv*. 2015;5:21125–31. <http://xlink.rsc.org/?DOI=C5RA00374A>.
18. Mohamed SSY, Martínez S, Banchemo M, Manna L, Ronchetti S, Onida B. The role of the pH in the impregnation of spherical mesoporous silica particles with L-arginine aqueous solutions. *Int J Mol Sci*. 2021;22:13403. <https://www.mdpi.com/1422-0067/22/24/13403>.
19. Escax V, Delahaye E, Impéror-Clerc M, Beaunier P, Appay MD, Davidson A. Modifying the porosity of SBA-15 silicas by post-synthesis basic treatments. *Microporous Mesoporous Mater*. 2007;102:234–41.
20. Thommes M, Kaneko K, Neimark AV, Olivier JP, Rodríguez-Reinoso F, Rouquerol J, et al. Physisorption of gases, with special reference to the evaluation of surface area and pore size distribution (IUPAC Technical Report). *Pure Appl Chem*. 2015;87:1051–69. <https://www.degruyter.com/document/doi/10.1515/pac-2014-1117/html>.
21. Rimola A, Costa D, Sodupe M, Lambert J-F, Ugliengo P. Silica surface features and their role in the adsorption of biomolecules: computational modeling and experiments. *Chem Rev* [Internet]. 2013;113:4216–313. <https://pubs.acs.org/doi/10.1021/cr3003054>.
22. El Mourabit S, Guillot M, Toquer G, Cambedouzou J, Goettmann F, Grandjean A. Stability of mesoporous silica under acidic conditions. *RSC Adv* [Internet]. 2012;2:10916. <https://xlink.rsc.org/?DOI=c2ra21569a>.
23. Ralph K Iler. *The chemistry of silica: solubility, polymerization, colloid and surface properties and biochemistry of silica*. United Kingdom: Wiley; 1979.
24. Ek S, Root A, Peussa M, Niinistö L. Determination of the hydroxyl group content in silica by thermogravimetry and a comparison with <sup>1</sup>H MAS NMR results. *Thermochim Acta*. 2001;379:201–12. <https://linkinghub.elsevier.com/retrieve/pii/S0040603101006189>.
25. De Farias RF, Airoidi C. Thermogravimetry as a reliable tool to estimate the density of silanols on a silica gel surface. *J Therm Anal Calorim*. 1998;53:751–6.
26. Shenderovich IG, Buntkowsky G, Schreiber A, Gedat E, Sharif S, Albrecht J, et al. Pyridine-<sup>15</sup>N a mobile NMR sensor for surface acidity and surface defects of mesoporous silica. *J Phys Chem B*. 2003;107:11924–39. <https://pubs.acs.org/doi/10.1021/jp0349740>.
27. Yildirim A, Ozgur E, Bayindir M. Impact of mesoporous silica nanoparticle surface functionality on hemolytic activity, thrombogenicity and non-specific protein adsorption. *J Mater Chem B*. 2013;1:1909. <https://xlink.rsc.org/?DOI=c3tb20139b>.
28. Pavan C, Tomatis M, Ghiazza M, Rabolli V, Bolis V, Lison D, et al. In search of the chemical basis of the hemolytic potential of silicas. *Chem Res Toxicol*. 2013;26:1188–98. <https://pubs.acs.org/doi/10.1021/tx400105f>.
29. Shi J, Hedberg Y, Lundin M, Odnevall Wallinder I, Karlsson HL, Möller L. Hemolytic properties of synthetic nano- and porous silica particles: The effect of surface properties and the protection by the plasma corona. *Acta Biomater*. 2012;8:3478–90. <https://linkinghub.elsevier.com/retrieve/pii/S1742706112001717>.
30. Bolis V, Fubini B, Marchese L, Martra G, Costa D. Hydrophilic and hydrophobic sites on dehydrated crystalline and amorphous silicas. *J Chem Soc Faraday Trans*. 1991;87:497. <http://xlink.rsc.org/?DOI=f9918700497>.
31. Gazzano E, Ghiazza M, Polimeni M, Bolis V, Fenoglio I, Attanasio A, et al. Physicochemical determinants in the cellular responses to nanostructured amorphous silicas. *Toxicol Sci*. 2012;128:158–70. <https://academic.oup.com/toxsci/article-lookup/doi/10.1093/toxsci/kfs128>.
32. Bolis V, Busco C, Ugliengo P. Thermodynamic study of water adsorption in high-silica zeolites. *J Phys Chem B*. 2006;110:14849–59. <https://pubs.acs.org/doi/10.1021/jp061078q>.